CellPress

Trends in Neurosciences

Review

Toward individualized connectomes of brain morphology

Jinhui Wang[1,2,3,*] and Yong He[4,5,6,*]

The morphological brain connectome (MBC) delineates the coordinated patterns of local morphological features (such as cortical thickness) across brain regions. While classically constructed using population-based approaches, there is a growing trend toward individualized modeling. Currently, the methods for individualized MBCs are varied, posing challenges for method selection and cross-study comparisons. Here, we summarize how individualized MBCs are modeled through low-order methods (correlation-, divergence-, distance-, and deviation-based methods) describing relations in brain morphology, as well as high-order methods capturing similarities in these low-order relations. We discuss the merits and limitations of different methods, examining them in the context of robustness, reproducibility, and reliability. We highlight the importance of elucidating the cellular and molecular mechanisms underlying the individualized connectome, and establishing normative benchmarks to assess individual variation in development, aging, and neuropsychiatric disorders.

Highlights

The morphological brain connectome (MBC) can be mapped at an individual level from a single structural MRI scan.

Individualized MBCs can be modeled using both low-order and high-order methods, each of which has its own advantages and disadvantages.

Individualized MBCs exhibit nontrivial topological properties such as small-worldness, modular organization, and hubs with high robustness, reproducibility, and reliability.

Future work is needed to elucidate the cellular and molecular basis of individualized MBCs and to establish normative benchmarks to better understand individual variations in healthy and diseased conditions.

Individualized morphological brain networks: a novel approach to the human brain connectome

It is generally accepted that the human brain functions as a complex, interconnected network (i.e., a **connectome**) [1] (see Glossary) to facilitate behavior and cognition [2,3]. This notion led to the emergence of the field of network neuroscience, which approaches brain structure and function from an integrative perspective by mapping, analyzing, and modeling the elements of the brain and their interactions [4]. In the past two decades, network neuroscience has significantly advanced our understanding of the architecture, organization, and underlying principles of the wiring diagram in the human brain [5–8].

Currently, there are two main methods for mapping the human brain connectome *in vivo*: structural connectivity, typically derived from diffusion MRI using fiber tractography, and functional connectivity, estimated as the temporal synchronization of neural activity recorded by functional imaging techniques such as functional MRI. Structural connectivity corresponds to the physical axonal pathways responsible for neuronal signaling and communication in the brain, whereas functional connectivity is derived from statistical descriptions of time series and is highly time-dependent [9]. In recent years, the MBC has received considerable attention for mapping the morphological connectivity patterns of the brain in healthy and diseased populations. Morphological connectivity is defined as the statistical interdependence of local morphological features between regions (Box 1). Initial studies estimated inter-regional morphological connectivity by correlating specific morphological features, such as cortical thickness or gray matter volume derived from structural MRI data, across participants [10–14]. However, these population-based MBC methods provide only one network for a group of participants, limiting their broader applicability. Recognizing this limitation, the field of the MBC is currently experiencing a pivotal shift from population-based

[1]Institute for Brain Research and Rehabilitation, South China Normal University, Guangzhou 510631, China
[2]Guangdong Key Laboratory of Mental Health and Cognitive Science, South China Normal University, Guangzhou 510631, China
[3]Center for Studies of Psychological Application, South China Normal University, Guangzhou 510631, China
[4]IDG/McGovern Institute for Brain Research, Beijing Normal University, Beijing 100875, China
[5]National Key Laboratory of Cognitive Neuroscience and Learning, Beijing Normal University, Beijing 100875, China
[6]Beijing Key Laboratory of Brain Imaging and Connectomics, Beijing Normal University, Beijing 100875, China

*Correspondence:
jinhui.wang.1982@m.scnu.edu.cn (J. Wang) and yong.he@bnu.edu.cn (Y. He).

 https://doi.org/10.1016/j.tins.2023.11.011

Box 1. Major features of brain morphology

Recent advances in automated image analysis techniques allow a large number of morphological features to be extracted from a single structural MRI scan. Specifically, using voxel- and surface-based morphometry methods, researchers can extract multiple morphological features at tens of thousands of points across the cortical mantle, such as gray matter volume, cortical thickness, surface area, sulcal depth, and fractal dimension (Figure I). Gray matter volume in MRI scans is typically defined as the amount of gray matter between the gray–white interface and the pia mater. Cortical thickness measures the distance between the gray–white interface and the gray–cerebrospinal fluid interface (i.e., the pial surface) and reflects the arrangement, size, and density of neurons, neuroglia, and nerve fibers. Surface area is defined as the area of the exposed cortical pial surface and hidden area of the cortex within the sulci and is thought to be driven by the number of cortical columns. Sulcal depth describes the distance from the central surface to the hemispheric hull surface and characterizes the folded structure of the cortex. Fractal dimension is considered to be a combination of the frequency of cortical folding, sulcal depth, and the convolution of gyral shape and quantifies the complexity of cortical folding. Notably, the definitions and calculation methods for these morphological features can vary in the literature.

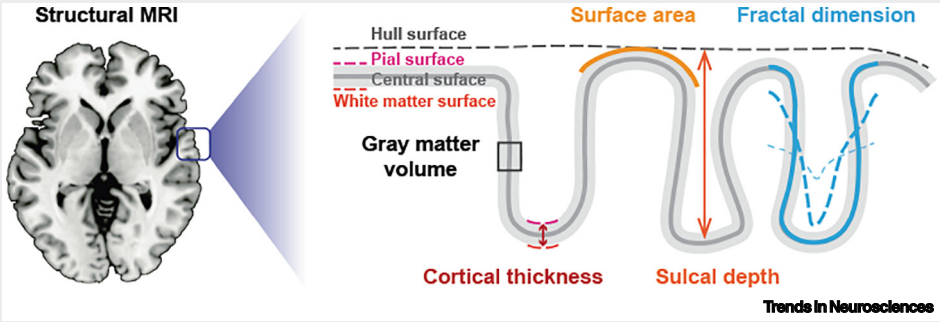

Figure I. Schematic diagram of various features of brain morphology.

approaches to individualized modeling. This transition offers unparalleled opportunities to study interindividual variance in the coordinated patterns of brain morphology in health and disease.

Compared with individual-based structural connectivity and functional connectivity, individualized MBCs are particularly suitable for studies aimed at identifying biomarkers for development, aging, and brain disorders. This is because (i) individualized MBCs have been often shown to have high **robustness**, **reproducibility**, and **reliability** [15–28]; (ii) individualized MBCs are probably the simplest, fastest, and most cost-effective MRI-based brain networks and therefore have potentially greater utility in multicenter, large-sample collaborative studies; and (iii) structural MRI has unique advantages over diffusion and functional MRI in terms of its widespread availability, high signal-to-noise ratio, high spatial resolution, and relative insensitivity to artifacts (e.g., head motion). Although the biological significance of individualized MBCs is not fully understood, accumulating evidence points to the important role of genetic, cytoarchitectonic, and chemoarchitectonic factors in the formation and shaping of individualized MBCs [20,25–27,29,30]. Moreover, individualized MBCs recapitulate, to some extent, the structural networks of axonal white matter tracts [20,27], functional networks of synchronized brain activity [31], and networks of coordinated development [29]. These findings support the biological validity of individualized MBCs.

In this review, we aim to provide a systematic overview of state-of-the-art progress in the field of individualized MBCs. We highlight in particular methods for individualized MBCs, given that one of the main challenges in the field is estimating inter-regional morphological connectivity from a single MRI scan. We also summarize the robustness, reproducibility, and reliability of individualized MBCs. Finally, we conclude with open questions and directions for future research.

Glossary

Characteristic path length: a measure of network integration that quantifies the overall routing efficiency of a network by calculating the average shortest path length between all pairs of nodes in the network.
Clustering coefficient: a measure of network segregation that quantifies the extent of local 'cliquishness' of nodes in a network.
Connectome: in the context of human brain studies, the connectome refers to a comprehensive map detailing the structural, functional, and morphological connectivity pattern of the brain that can be derived macroscopically from advanced multimodal MRI technologies.
Graph: a mathematical representation of a network consisting of nodes linked by edges.
Hubs: nodes that are highly connected and occupy a central position in a network.
Local efficiency: a measure of segregation that reflects the capacity of a network for modular information processing or fault tolerance.
Modularity: the extent to which the edges of a network tend to link nodes within the same module, which is a group of densely interconnected nodes that have few connections to nodes outside their group.
Parallel efficiency: the ability of a network to transfer information between nodes through multiple concurrent paths.
Parcellation: a division of the brain into a number of anatomically or functionally distinct regions.
Reliability: the consistency of results when the same evaluation is administered to the same participants at different times.
Reproducibility: the consistency of results when the same evaluation is administered to different participants.
Rich-club: a phenomenon in which highly connected nodes tend to be more closely interconnected than would be expected by chance.
Robustness: the consistency of results when the same evaluation is performed on the same participants with different implementation details, such as different analytical methods or parameters.
Small-worldness: a combination of high clustering and short path length, allowing both segregated and integrated information processing within a network.

Basic concepts of brain networks

A network consists of a set of nodes, as well as edges that connect the nodes. In the context of brain networks, nodes typically denote **parcellation** units within the brain (e.g., regions, vertices, or voxels), and edges represent brain connectivity between nodes, as derived from various neuroimaging techniques. Once a brain network is constructed, it can be modeled as a **graph** and further topologically characterized using graph theory-based approaches. The graph theory-based framework provides a set of well-defined metrics to quantify the system-level organization of a network or graph [6,32,33].

Methods for individualized MBCs

To date, several methods have been developed to construct individualized MBCs, which can be divided into two categories: low-order and high-order. The low-order methods represent pairwise relations in local morphological features between brain nodes (Figure 1), while the high-order methods describe similarities between low-order morphological relations (Figure 2). Currently, research on individualized MBCs has been predominantly based on low-order methods, which can

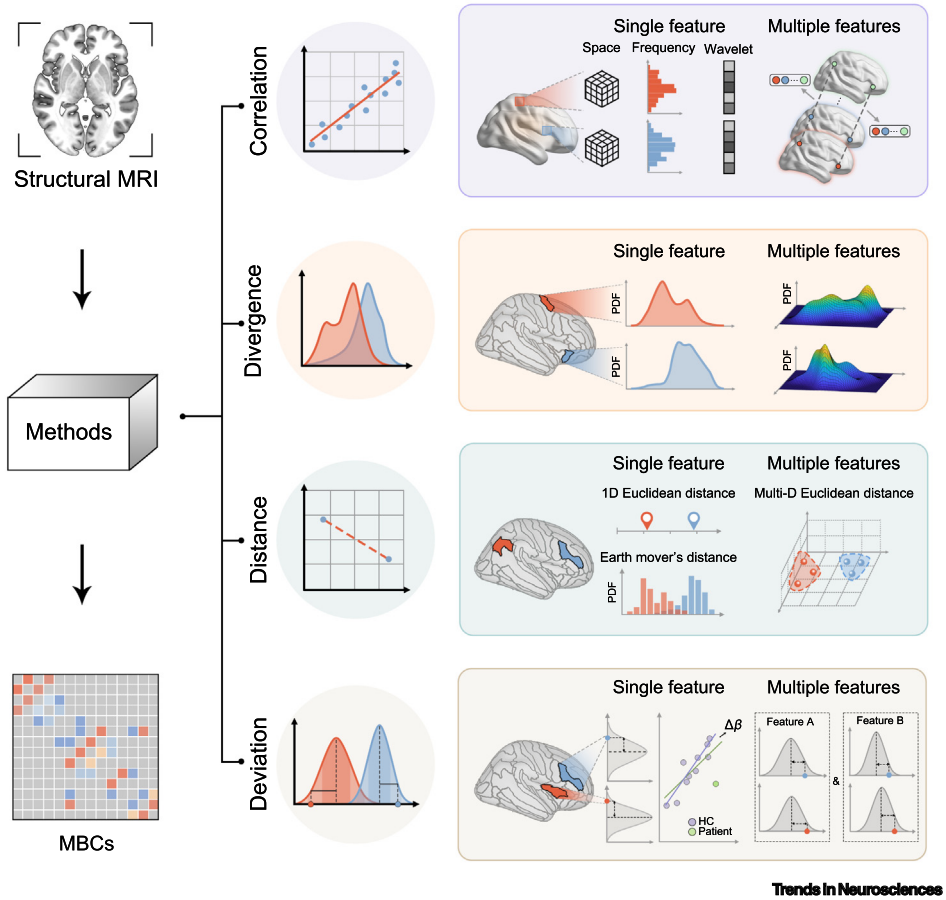

Figure 1. Overview of low-order methods for individualized MBCs. Low-order individualized MBCs represent pairwise relations in local morphological features between brain nodes. They can be constructed using four classes of methods: correlation-based, divergence-based, distance-based, and deviation-based methods. Within each class, methods also differ in the number of morphological features used to estimate inter-regional morphological relations (single vs. multiple features). Abbreviations: HC, healthy control; MBCs, morphological brain connectomes; PDF, probability density function.

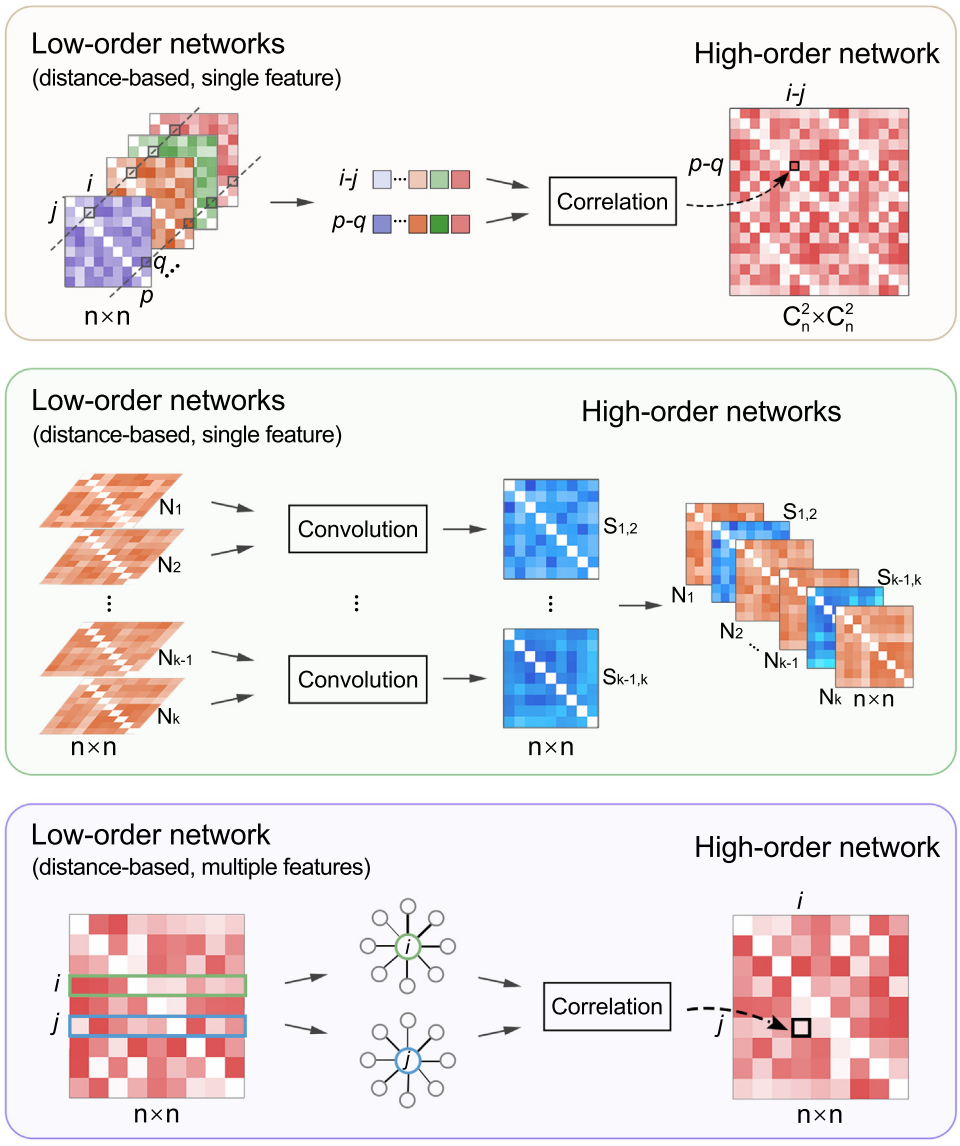

Figure 2. Overview of high-order methods for individualized morphological brain connectomes (MBCs). High-order individualized MBCs describe similarities between low-order morphological relations. They can be derived by analyzing the interactions of low-order morphological relations between different pairs of brain regions (top row), by convolving different pairs of low-order individualized MBCs (middle row), or by estimating the correlations of regional profiles of low-order morphological relations between brain regions (bottom row).

be further categorized into four classes according to the measure utilized to estimate inter-regional morphological connectivity: correlation-based, divergence-based, distance-based, and deviation-based. Within each class, the methods also differ in the number of morphological features being used (single vs. multiple).

Correlation-based methods

In statistical analyses, Pearson correlation is a widely used method for quantifying the extent to which two variables have a linear relationship. When using Pearson correlation to detect inter-

regional morphological connectivity, the main challenge is how to define the samples or observations for which the correlation is calculated. Two subclasses of methods have been developed to address this challenge: one defines the samples as discrete representations of a single morphological feature in different domains (space, frequency, or wavelet) [15,21,34,35], and the other treats different morphological features as observations [19,20,26].

In an initial study, individualized MBCs were constructed using a correlation-based, single-feature method[i] [15]. In this study, the brain was parcellated into thousands of cubes (27 voxels per cube), between which the morphological connectivity was estimated by calculating the Pearson correlation of gray matter volume across intracube voxels. However, as the cubes are defined in individual native space, the resulting networks have a different number of network nodes between participants. In addition, the rigid extraction of the cubes may not correspond well to functionally or anatomically homogeneous regions of the brain. As a remedy, a cube-to-region transformation is typically applied to improve comparability between participants and facilitate interpretation of results [36]. Subsequently, a simpler method was proposed to generate individualized MBCs at the regional level based on prior brain parcellations [34]. Given the variability in regional sizes, the Pearson correlation is calculated across vertex frequencies in 30 uniform bins of regional gray matter volume to determine inter-regional morphological connectivity. This method is less computationally demanding than the previous method and more flexible in the definition of network nodes. However, both methods overlook the unique connectivity of different voxels or vertices within cubes or regions. To address this, researchers have developed a voxel-level method that estimates the morphological connectivity between voxels by calculating the Pearson correlation across a set of voxel-wise wavelet coefficients derived from applying a wavelet transform to a gray matter volume map[ii] [21]. The wavelet transform, a multiresolution technique, can decompose the energy of a signal into a hierarchically organized group of scales [37] and has proven to be an efficient tool for the signal representation of structural MRI data [38]. Notably, the wavelet transform can also be used to generate individualized MBCs between white matter regions [35].

In contrast to the methods that estimate morphological connectivity using discrete representations of a single morphological feature, the second subclass of correlation-based methods calculates the Pearson correlation across multiple morphological features to infer morphological connectivity. Previous research suggests that different morphological features have unique cellular mechanisms and genetic underpinnings [39,40]. Therefore, integrating multiple morphological features may be beneficial for the accurate mapping of individualized MBCs. There are several correlation-based, multifeature methods currently available [19,20,26]. These methods differ mainly in how they extract as many morphological features as possible to estimate morphological connectivity. Specifically, an earlier study used seven features derived from the surface-based morphometric analysis of structural MRI data [19]. Later studies incorporated more features, either by adding an additional data modality of diffusion MRI (ten features) [20] or through radiomics-based analysis of structural MRI data[iii] (25 features) [26]. It should be noted that these multifeature methods are based on a single summary statistic for each morphological feature per region, thereby omitting detailed voxel- or vertex-level connectivity information. In addition, these methods require a potentially unrealistic standardization by forcing each morphological feature to be equally variable across regions.

Divergence-based methods

There are several divergence measures in mathematical statistics and probability theory to determine the dissimilarity between two probability distributions. The core principle of divergence-based methods for individualized MBCs involves estimating a probability density function (PDF) from a morphological feature within a brain region. The dissimilarity between regional PDFs is then quantified using different divergence measures. Initial studies used gray matter volume to

estimate the PDFs and Kullback–Leibler divergence to quantify PDF dissimilarity [16,17]. However, gray matter volume is thought to reflect a composite of several factors, including thickness, area, and folding. Consequently, individualized MBCs constructed on the basis of gray matter volume overlook the nuanced connectivity data inherent in distinct, finely defined morphological features. Kullback–Leibler divergence has poor mathematical properties, such as asymmetry and unboundedness. Considering these issues, divergence-based methods have been subsequently extended from gray matter volume to several cortical surface-based morphological features that capture specific aspects of brain morphology (e.g., cortical thickness, fractal dimension, gyrification index, and sulcal depth) and from the Kullback–Leibler divergence to the Jensen–Shannon divergence (a symmetric variant of the Kullback–Leibler divergence with finite values) [24]. Notably, individualized MBCs derived from different surface-based morphological features exhibit distinct connectivity patterns [24], sensitivities to disease-related alterations [41], and trajectories across the adult lifespan [42]. These findings underscore the need to develop methods that can integrate different morphological features for a more accurate mapping of individualized MBCs. Along these lines, a recent study introduced a multivariate strategy by formulating a multidimensional distribution of several morphological features per region[iv] [27]. Specifically, a *k*-nearest neighbor approach is used to compute multivariate Kullback–Leibler divergence from vertex-level data, considering the computational demands and suboptimal results of multivariate PDF estimation [43]. In addition to divergence measures, mutual information is also used to quantify the similarity between regional PDFs of gray matter volume after dimension reduction by principal component analysis [18].

Distance-based methods

Mathematically, there are many distance functions to quantify the dissimilarity between two variables. The simplest distance function is the Euclidean distance between two points in a 1D coordinate system, defined as the absolute difference in their coordinates. Using this function or its variant (i.e., the square of the difference between two points), previous studies have developed methods to construct individualized MBCs based on the regional mean of specific morphological features such as cortical thickness, sulcal depth, and curvature [44–46]. However, such a simplistic representation of inter-regional dissimilarity may introduce biases into the resulting networks, as it does not account for intra-regional morphological patterns or inter-voxel/vertex relationships in different regions. These challenges can be mitigated by advanced distance functions rooted in data distributions, such as the earth mover's distance [47], or by determining distance at the voxel/vertex level [48]. Beyond 1D distance estimates based on a single morphological feature, inter-regional dissimilarity can also be assessed in a multidimensional space spanning different morphological features. In this context, two studies constructed individualized MBCs by calculating the Euclidean [22] and Mahalanobis [49] distances between regional vectors comprising six and five morphological features, respectively.

Deviation-based methods

Deviation-based methods for individualized MBCs are based on the rationale that the deviation of an observation from a reference distribution can be used to estimate the similarity between observations. Specifically, for a given reference distribution, the deviation of an observation is quantified by a Z score, which is calculated as the difference between the observation and the mean of the reference distribution divided by the standard deviation of the reference distribution. The similarity between two observations can then be expressed by their Z scores. To date, several studies have adopted this strategy to construct individualized MBCs in which the observations represent mean cortical thickness, surface area, curvature, or volume within brain regions [50–55]. A main difference between these studies lies in the formulas used to determine the similarity between two Z scores, which include the maximum of their absolute values [50], the average of their absolute

values [51,52], and the inverse of the exponential function derived from the square of their difference [53–55]. In addition, the definition of the reference distribution varies across studies. Specifically, most studies define the reference distribution for each brain region based on data from all healthy subjects in the control group [50,51,53–55]. In contrast, one study defined the reference distribution using vertex-wise data within each brain region [52]. This discrepancy leads to different interpretations of the Z scores, namely, the deviation of one brain region of one individual from the same brain region in healthy controls or the deviation of one brain region relative to another brain region within the same individual. In addition to inferring inter-regional morphological connectivity based on deviations in local brain morphology, a recent study constructed individualized MBCs by examining the differences in inter-regional morphological connectivity before and after the addition of an extra patient to a control group of healthy subjects [56]. These differences follow a symmetric distribution, termed the 'volcano distribution', and can be transformed into Z scores, indicating the impact of the added patient on the inter-regional morphological connectivity estimated from the reference group of healthy controls. It is worth noting that the core of this class of methods requires the construction of a robust normative reference model using a large structural MRI dataset.

High-order individualized MBCs

The methods for constructing individualized MBCs discussed thus far are considered low-order methods, focusing only on pairwise relations between brain nodes in local brain morphology. Currently, several methods have been introduced to develop high-order individualized MBCs based on low-order networks. In an initial study, high-order individualized MBCs were formulated by examining the interplay of low-order morphological relations between different pairs of brain nodes [46]. Specifically, four low-order, distance-based, single-feature individualized MBCs were first constructed. Across these networks, the Pearson correlation was then computed for the morphological relations between different pairs of brain regions, capturing the covariance of morphological relations between two regions with respect to another pair. In a subsequent study, a brain multiplex was used to model the interactions between four low-order, distance-based, single-feature individualized MBCs by convolving each pair of the networks [57]. The convolution blends two networks together and represents their degree of overlap as one network is shifted over the other. In addition, this study introduced a deep multilevel network architecture to extract high-order morphological network information, where each level integrates the similarity networks of all network pairs in the previous level. Finally, a recent study built high-order individualized MBCs by computing the inter-regional linear correlation in the regional connectivity profiles of low-order, distance-based, multifeature MBCs [23].

Topological architecture of individualized MBCs

Regardless of the specific method used, graph-based analyses of the resulting individualized MBCs consistently reveal non-trivial topological properties, including **small-worldness**, high **parallel efficiency**, **modularity**, **rich-club** architecture, and **hubs** [15–22,24,26,27]. These findings suggest that the edges of individualized MBCs are wired in specific and partly consistent ways. The brain-wide network is characterized by gradual transitions of inter-regional morphological connectivity across the cortical mantle along a principal axis anchored by the motor and sensory cortices at its extremities and the association cortices centrally [25]. Presumably, this wiring pattern may have evolved due to natural selection pressures favoring cost efficiency. Notably, despite the shared topological structure, initial quantitative comparisons have revealed discernible differences between the MBCs resulting from different methods. For instance, the small-worldness property of individualized MBCs derived from a low-order, distance-based, multifeature method is apparently higher than that of individualized MBCs built from a low-order, correlation-based, single-feature method [22]. This raises a key question: which method

is optimal for the construction of individualized MBCs? Deeper insights into this question can be gained by evaluating and contrasting the robustness, reproducibility, and reliability of each method.

Robustness, reproducibility, and reliability of individualized MBCs

Following the formulation of methods for individualized MBCs, several studies have delved deeper into examining the networks with respect to their robustness to methodological variation, reproducibility across participants or datasets, and reliability between scans and rescans (Table 1). Individualized MBCs consistently show high robustness, reproducibility, and reliability, regardless of the specific method used. For example, individualized MBCs derived from low-order, correlation-based, multifeature methods are robust to the use of different feature sets [20,25,26]. Nevertheless, the evidence so far suggests that the performance of different methods varies: (i) for robustness, low-order, divergence-based, multifeature methods appear to outperform low-order, correlation-based, multifeature methods [27]; (ii) for reproducibility, low-order, divergence-based, multifeature methods outperform low-order, divergence-based, single-feature methods [27]; and (iii) for reliability, Jensen–Shannon divergence seems superior to Kullback–Leibler divergence, and cortical folding-related morphological features are superior to cortical thickness within the realm of low-order, divergence-based, single-feature methods [24,28]. In addition, for low-order, divergence-based, single-feature methods, certain analytical choices, such as performing spatial smoothing, using a high-resolution brain parcellation atlas, and using a proportional thresholding procedure, can further improve reliability [24,28].

Concluding remarks and future perspectives

Although individualized MBCs have received increasing attention in recent years, the field is still in its infancy. As discussed next, several fundamental questions remain to be addressed (see also Outstanding questions).

Outstanding questions

What are the precise cellular and molecular mechanisms underlying individualized MBCs?

What is the relationship among the morphological, structural, and functional connectomes of the brain? Does the relationship among the connectomes change over the course of normal development and aging or during brain disorders, and if so, how?

Can individualized MBCs be modulated by drugs or neuromodulation techniques (e.g., transcranial magnetic stimulation)? What are the functional changes that occur following the modulation?

Individual skill acquisition and training can lead to plastic changes in individualized MBCs. What are the mechanisms underlying these changes?

How do different sources of methodological noise, such as confounds associated with multi-site datasets and in-scanner head motion, affect the network architecture of individualized MBCs?

Table 1. A summary of studies evaluating the robustness, reproducibility, and/or reliability of individualized MBCs

Refs	Method			Approach to assess		
	Order	Measure	Feature	Robustness	Reproducibility	Reliability
[15]	Low	Correlation	Single			Two scans (interval: <6 months)
[21]	Low	Correlation	Single	Wavelet scale, network threshold, and network type		Two scans (interval: 1 h)
[19]	Low	Correlation	Multiple			Multiple scans
[20]	Low	Correlation	Multiple	Feature sets and brain parcellation	Within a dataset and between two datasets	
[25]	Low	Correlation	Multiple	Feature sets and brain parcellation	Between five datasets	
[26]	Low	Correlation	Multiple	Feature sets and brain parcellation	Within a dataset	Multiple scans
[16]	Low	Divergence	Single		Within a dataset	Two scans (interval: <1 day)
[17]	Low	Divergence	Single	Spatial smoothing, brain parcellation, and network type		Two scans (interval: ~6 weeks)
[24]	Low	Divergence	Single	Brain parcellation and similarity measure	Within a dataset	Two scans (interval: ~6 weeks)
[28]	Low	Divergence	Single			Multiple scans in different sites
[18]	Low	Divergence	Single		Within a dataset	Two scans (interval: ~1 month)
[27]	Low	Divergence	Multiple	Brain parcellation and noisy features	Within a dataset and between two datasets	
[22]	Low	Distance	Multiple			Two scans (interval: <3 months)
[23]	High	Distance	Multiple			Two scans (interval: 1 h)

First, given the plethora of methods currently available for individualized MBCs, a practical concern is how these methods correlate with each other. It remains largely undetermined whether each method provides unique or similar insights into the network organization of the human brain. To date, only a handful of studies have compared some of these methods from different perspectives, such as their performance in disease classification and diagnosis, alignment with axonal tract-tracing connectivity, or reliability [22,24,27,28,46,57–59]. However, these studies have mainly focused on within-class comparisons. A significant gap remains in conducting systematic exploration of the similarities and differences between the different methods tailored for individualized MBCs. More comparative studies are warranted to address this fundamental question using both simulated and empirical data. To facilitate such studies, it is important to develop user-friendly, open-source, freely available toolboxes capable of integrating the existing methods and possibly reach a standardized pipeline for individualized MBC studies.

Second, given the nascent nature of individualized MBCs, a pertinent question arises: how do these networks correlate with other types of established brain networks, such as structural and functional networks? Although there are some studies on this topic [20,25,27,31,60], the intricate inter-relationships remain largely unexplored. Therefore, findings and methods for the construction and characterization of other types of brain networks should be carefully evaluated and adapted to the context of individualized MBCs. In the future, a holistic understanding of the inter-relationships may benefit from an integrated analysis of multimodal and multiscale brain networks [61].

Third, structural MRI, like functional and diffusion MRI, is susceptible to noise from a variety of sources. Among these, in-scanner head motion stands out as a predominant concern in

Box 2. Individualized MBCs during development and aging

Brain morphology undergoes significant changes throughout the human lifespan [70]. These changes inevitably lead to the remodeling of coordinated patterns in brain morphology. Due to advances in the methodology of individualized MBC modeling, researchers can now explore interindividual variation in the coordination patterns of brain morphology during development and aging (Table I). Several studies have reported age-related changes in individualized MBCs at different levels, including inter-regional morphological connectivity, nodal centrality, and overall topological structure [16,42,71–73]. These changes are modulated by several factors, such as sex [73] and anatomical distance between brain regions [42]. Interestingly, **local efficiency** is consistently found to decrease with age across the adult lifespan [16,42,73]. In addition to tracking the trajectory of individualized MBCs with age, a few studies have used individualized MBCs to predict brain age [27,73,74] and to discriminate between preterm and full-term infants [74]. Individualized MBCs have been shown to successfully predict brain age regardless of the age range of participants [27,73,74]. Notably, low-order, divergence-based, multifeature methods show superior predictive performance compared to low-order, correlation-based, multifeature methods [27].

Table I. A summary of individualized MBC studies on development and aging

Refs	Participant	Age	Method		
			Order	Measure	Feature
[16]	21 adults	22–61 years	Low	Divergence	Single
[71]	241 infants	37–44 weeks postmenstrual age	Low	Correlation	Multiple
[72]	1427 adults	20–89 years	Low	Divergence	Single
[73]	812 adults	25.8–85.1 years	Low	Correlation	Single
[42]	650 adults	18–88 years	Low	Divergence	Single
[74]	105 neonates	38–45 weeks postmenstrual age	Low	Correlation	Multiple
[27]	960 adults 655 subjects	21–35 years 8–21 years	Low	Divergence and correlation	Single and multiple

Box 3. Individualized MBCs in brain disorders

Individualized MBCs have been used to study various brain disorders (Table I). These studies are involved in delineating abnormal organization, identifying biological subtypes, predicting treatment outcomes, and classifying disease states. In the following, we use Alzheimer's disease as an illustrative example, as it is among the most studied diseases for the clinical application of individualized MBCs. Despite considerable variation in methods and samples across studies, it has been consistently found that individualized MBCs in Alzheimer's disease shift toward a more randomized topological organization (i.e., reduced **clustering coefficient** and/or **characteristic path length**), irrespective of disease stage [75–78]. Furthermore, the more randomized topological organization of individualized MBCs occurs before symptom onset [78], accounts for cognitive deficits [76,79], predicts faster cognitive decline [80], and is associated with an increased risk of progression [77]. In addition, individualized MBCs have been shown to be able to classify patients at different disease stages from controls and to identify and separate different subgroups [22,57,58,81–83]. Notably, compared to solely utilizing regional morphology or inter-regional structural or functional connectivity, the integration of additional individualized MBCs accounts for a greater proportion of the variance in cognitive decline of patients and improves the efficacy of diagnostic and prognostic models across disorders [47,49,76,82,84–86]. Finally, high-order methods for individualized MBCs show superiority over low-order methods in disease classification [46,57–59], and divergence- and distance-based methods show greater sensitivity than correlation-based methods in detecting alterations associated with attention-deficit/hyperactivity disorder [87].

Table I. A summary of individualized MBC studies on brain disorders

Disease	Method		
	Order (Refs)	Measure (Refs)	Feature (Refs)
Alzheimer's disease	Low: [22,75–83,88] High: [57,58]	Correlation: [75–81] Divergence: [82,83,88] Distance: [22,57,58]	Single: [57,58,75–80,82,83,88] Multiple: [22,81]
Schizophrenia	Low: [53,56,85,89–93]	Correlation: [91,93] Divergence: [85,89,90,92] Deviation: [53,56]	Single: [53,56,85,89,90,92,93] Multiple: [91]
Major depressive disorder	Low: [51,94–100] High: [59]	Correlation: [94,96–98,100] Divergence: [95,99] Distance: [59] Deviation: [51]	Single: [51,94,95,97–100] Multiple: [96]
Autism spectrum disorder	Low: [47,101–104] High: [46]	Divergence: [102–104] Distance: [46,47,101]	Single: [47,101–104]
Bipolar disorder	Low: [53,93,105,106]	Correlation: [93,105] Divergence: [106] Deviation: [53]	Single: [53,93,105,106]
Multiple sclerosis	Low: [84,86,107,108]	Correlation: [84,86,107] Divergence: [108]	Single: [84,86,107,108]
Temporal lobe epilepsy	Low: [50,109–111]	Correlation: [109–111] Deviation: [50]	Single: [109] Multiple: [50,110,111]
Attention-deficit/hyperactivity disorder	Low: [49,87,112]	Correlation: [87,112] Divergence: [87] Distance: [49,87]	Single: [87,112] Multiple: [49]
Social anxiety disorder	Low: [98,113,114]	Correlation: [98,113] Divergence: [114]	Single: [98,113,114]
Parkinson's disease	Low: [115,116]	Divergence: [115,116]	Single: [115,116]
Post-traumatic stress disorder	Low: [117,118]	Correlation: [117,118]	Single: [117,118]
Stroke	Low: [41]	Divergence: [41]	Single: [41]
Neuromyelitis optica spectrum disorder	Low: [108]	Divergence: [108]	Single: [108]
Obsessive-compulsive disorder	Low: [54]	Deviation: [54]	Single: [54]

neuroimaging. Previous research has shown that in-scanner head motion can significantly influence inter-regional relationships in functional [62,63], structural [64], and population-based morphological [65] brain networks. However, the impact of in-scanner head motion on individualized MBCs remains largely unexplored. In addition to in-scanner head motion, site/scanner-related effects are another important source of noise in multicenter MRI studies. This issue is particularly relevant to individualized MBCs, which are suitable for multicenter, large-scale collaborative studies. Although numerous statistical and deep learning harmonization methods have been developed to control for site/scanner-related effects [66], it is largely unknown whether these methods work effectively on individualized MBCs. Finally, it should be noted that standardization of morphological estimates from structural MRI images is still in progress. Several previous studies have shown systematic differences in morphological estimates between different software packages [67–69], which may further affect downstream individualized MBCs. Elucidation of these effects is crucial for the reliable mapping of individualized MBCs by developing effective strategies to mitigate such influences.

Fourth, to biologically understand individualized MBCs, several studies have associated them with various publicly accessible attributes of cortical microarchitecture, such as gene expression, cytoarchitectonic classification, and myelin content [20,25–27,29,30]. However, whether these associations are unique to individualized MBCs or are shared with structural and functional brain networks is largely unknown. Addressing this fundamental question is essential for understanding the nature of individualized MBCs. Beyond the exploration of macro–micro-coupling, more tangible and compelling evidence for the neurobiological basis of individualized MBCs may emerge from research comparing the morphological connectivity of neurons with neuronal axonal projections. With the rapid development of modern molecular techniques, such investigations are on the horizon.

Finally, the high robustness, reproducibility, and reliability of individualized MBCs give them significant potential for detecting interindividual variation and identifying diagnostic and prognostic biomarkers in pathological scenarios. As a result, individualized MBCs are increasingly being used in the fields of brain development and aging (Box 2), as well as in various neurological and psychiatric disorders (Box 3). Further studies should take full advantage of the widespread availability of large structural MRI datasets to chart robust MBC trajectories across the lifespan that will serve as a reference to detect individual differences, identify biological subtypes, and localize potential neuromodulation targets for personalized medicine.

Acknowledgments

This work was supported by the National Natural Science Foundation of China (Grant Nos. 82021004 and 81922036) and the National Social Science Foundation of China (No. 20&ZD296). We thank Hao Wang, Yuqi Wang, and Ningke Han for their help in the preparation of the figures.

Declaration of interests

The authors declare no conflicts of interests.

Resources

[i]https://github.com/bettytijms/Single_Subject_Grey_Matter_Networks

[ii]www.nitrc.org/projects/mcwt/

[iii]https://github.com/YongLiuLab/R2SN_construction

[iv]https://github.com/isebenius/MIND

References

1. Sporns, O. *et al.* (2005) The human connectome: a structural description of the human brain. *PLoS Comput. Biol.* 1, e42
2. Park, H.J. and Friston, K. (2013) Structural and functional brain networks: from connections to cognition. *Science* 342, 1238411

3. Bressler, S.L. and Menon, V. (2010) Large-scale brain networks in cognition: emerging methods and principles. *Trends Cogn. Sci.* 14, 277–290
4. Bassett, D.S. and Sporns, O. (2017) Network neuroscience. *Nat. Neurosci.* 20, 353–364
5. Bullmore, E. and Sporns, O. (2012) The economy of brain network organization. *Nat. Rev. Neurosci.* 13, 336–349
6. Liao, X. *et al.* (2017) Small-world human brain networks: perspectives and challenges. *Neurosci. Biobehav. Rev.* 77, 286–300
7. Lynn, C.W. and Bassett, D.S. (2019) The physics of brain network structure, function and control. *Nat. Rev. Phys.* 1, 318–332
8. Seguin, C. *et al.* (2023) Brain network communication: concepts, models and applications. *Nat. Rev. Neurosci.* 24, 557–574
9. Preti, M.G. *et al.* (2017) The dynamic functional connectome: state-of-the-art and perspectives. *NeuroImage* 160, 41–54
10. Bassett, D.S. *et al.* (2008) Hierarchical organization of human cortical networks in health and schizophrenia. *J. Neurosci.* 28, 9239–9248
11. He, Y. *et al.* (2007) Small-world anatomical networks in the human brain revealed by cortical thickness from MRI. *Cereb. Cortex* 17, 2407–2419
12. Sanabria-Diaz, G. *et al.* (2010) Surface area and cortical thickness descriptors reveal different attributes of the structural human brain networks. *NeuroImage* 50, 1497–1510
13. Alexander-Bloch, A. *et al.* (2013) Imaging structural co-variance between human brain regions. *Nat. Rev. Neurosci.* 14, 322–336
14. Evans, A.C. (2013) Networks of anatomical covariance. *NeuroImage* 80, 489–504
15. Tijms, B.M. *et al.* (2012) Similarity-based extraction of individual networks from gray matter MRI scans. *Cereb. Cortex* 22, 1530–1541
16. Kong, X.Z. *et al.* (2015) Mapping individual brain networks using statistical similarity in regional morphology from MRI. *PLoS One* 10, e0141840
17. Wang, H. *et al.* (2016) Single-subject morphological brain networks: connectivity mapping, topological characterization and test-retest reliability. *Brain Behav.* 6, e00448
18. Jiang, J. *et al.* (2017) A novel individual-level morphological brain networks constructing method and its evaluation in PET and MR images. *Heliyon* 3, e00475
19. Li, W. *et al.* (2017) Construction of individual morphological brain networks with multiple morphometric features. *Front. Neuroanat.* 11, 34
20. Seidlitz, J. *et al.* (2018) Morphometric similarity networks detect microscale cortical organization and predict inter-individual cognitive variation. *Neuron* 97, 231–247 e237
21. Wang, X.H. *et al.* (2018) Mapping individual voxel-wise morphological connectivity using wavelet transform of voxel-based morphology. *PLoS One* 13, e0201243
22. Yu, K. *et al.* (2018) Individual morphological brain network construction based on multivariate Euclidean distances between brain regions. *Front. Hum. Neurosci.* 12, 204
23. Wang, X.H. *et al.* (2020) A unified framework for mapping individual interregional high-order morphological connectivity based on regional cortical features from anatomical MRI. *Magn. Reson. Imaging* 66, 232–239
24. Li, Y. *et al.* (2021) Surface-based single-subject morphological brain networks: effects of morphological index, brain parcellation and similarity measure, sample size-varying stability and test-retest reliability. *NeuroImage* 235, 118018
25. Yang, S. *et al.* (2021) Cortical patterning of morphometric similarity gradient reveals diverged hierarchical organization in sensory-motor cortices. *Cell Rep.* 36, 109582
26. Zhao, K. *et al.* (2021) Regional radiomics similarity networks (R2SNs) in the human brain: reproducibility, small-world properties and a biological basis. *Netw. Neurosci.* 5, 783–797
27. Sebenius, I. *et al.* (2023) Robust estimation of cortical similarity networks from brain MRI. *Nat. Neurosci.* 26, 1461–1471
28. Yin, G. *et al.* (2023) A comprehensive evaluation of multicentric reliability of single-subject cortical morphological networks on traveling subjects. *Cereb. Cortex* 33, 9003–9019
29. Wu, X. *et al.* (2023) Morphometric dis-similarity between cortical and subcortical areas underlies cognitive function and psychiatric symptomatology: a preadolescence study from ABCD. *Mol. Psychiatry* 28, 1146–1158
30. Li, Z. *et al.* (2023) Single-subject cortical morphological brain networks: phenotypic associations and neurobiological substrates. *NeuroImage* 283, 120434
31. Sun, L. *et al.* (2022) Structural insight into the individual variability architecture of the functional brain connectome. *NeuroImage* 259, 119387
32. Rubinov, M. and Sporns, O. (2010) Complex network measures of brain connectivity: uses and interpretations. *NeuroImage* 52, 1059–1069
33. He, Y. and Evans, A. (2010) Graph theoretical modeling of brain connectivity. *Curr. Opin. Neurol.* 23, 341–350
34. Li, C. *et al.* (2021) Large-scale morphological network efficiency of human brain: cognitive intelligence and emotional intelligence. *Front. Aging Neurosci.* 13, 605158
35. Wang, X.H. *et al.* (2022) Mapping white matter structural covariance connectivity for single subject using wavelet transform with T1-weighted anatomical brain MRI. *Front. Neurosci.* 16, 1038514
36. Batalle, D. *et al.* (2013) Normalization of similarity-based individual brain networks from gray matter MRI and its association with neurodevelopment in infants with intrauterine growth restriction. *NeuroImage* 83, 901–911
37. Bullmore, E. *et al.* (2004) Wavelets and functional magnetic resonance imaging of the human brain. *NeuroImage* 23, S234–S249
38. Canales-Rodriguez, E.J. *et al.* (2013) Statistical analysis of brain tissue images in the wavelet domain: wavelet-based morphometry. *NeuroImage* 72, 214–226
39. Winkler, A.M. *et al.* (2010) Cortical thickness or grey matter volume? The importance of selecting the phenotype for imaging genetics studies. *NeuroImage* 53, 1135–1146
40. Strike, L.T. *et al.* (2019) Genetic complexity of cortical structure: differences in genetic and environmental factors influencing cortical surface area and thickness. *Cereb. Cortex* 29, 952–962
41. Lv, Y. *et al.* (2021) Multiparametric and multilevel characterization of morphological alterations in patients with transient ischemic attack. *Hum. Brain Mapp.* 42, 2045–2060
42. Ruan, J. *et al.* (2023) Single-subject cortical morphological brain networks across the adult lifespan. *Hum. Brain Mapp.* 44, 5429–5449
43. Wang, Z. and Scott, D.W. (2019) Nonparametric density estimation for high-dimensional data—Algorithms and applications. *WIREs Comput. Stat.* 11, e1461
44. Dai, D. *et al.* (2012) Accurate prediction of AD patients using cortical thickness networks. *Mach. Vis. Appl.* 24, 1445–1457
45. Wee, C.Y. *et al.* (2013) Prediction of Alzheimer's disease and mild cognitive impairment using cortical morphological patterns. *Hum. Brain Mapp.* 34, 3411–3425
46. Soussia, M. and Rekik, I. (2017) High-order connectomic manifold learning for autistic brain state identification. In *Connectomics in Neuroimaging: First International Workshop, CNI 2017. Held in Conjunction with MICCAI 2017, Quebec City, QC, Canada, September 14, 2017, Proceedings* (1), pp. 51–59, Springer
47. Leming, M.J. *et al.* (2021) Single-participant structural similarity matrices lead to greater accuracy in classification of participants than function in autism in MRI. *Mol. Autism* 12, 34
48. Zheng, W. *et al.* (2015) Novel Cortical thickness pattern for accurate detection of Alzheimer's disease. *J. Alzheimers Dis.* 48, 995–1008
49. Wang, X.H. *et al.* (2018) Diagnostic model for attention-deficit hyperactivity disorder based on interregional morphological connectivity. *Neurosci. Lett.* 685, 30–34
50. Raj, A. *et al.* (2010) Network-level analysis of cortical thickness of the epileptic brain. *NeuroImage* 52, 1302–1313
51. Shin, J.H. *et al.* (2018) Multiple cortical thickness sub-networks and cognitive impairments in first episode, drug naive patients with late life depression: a graph theory analysis. *J. Affect. Disord.* 229, 538–545
52. Kim, H.J. *et al.* (2016) Using individualized brain network for analyzing structural covariance of the cerebral cortex in Alzheimer's patients. *Front. Neurosci.* 10, 394
53. Kim, S. *et al.* (2020) Altered cortical thickness-based individualized structural covariance networks in patients with schizophrenia and bipolar disorder. *J. Clin. Med.* 9, 1846

54. Yun, J.Y. *et al.* (2015) Neural correlates of response to pharmacotherapy in obsessive-compulsive disorder: individualized cortical morphology-based structural covariance. *Prog. Neuro-Psychopharmacol. Biol. Psychiatry* 63, 126–133
55. Yun, J.Y. *et al.* (2016) Individualized covariance profile of cortical morphology for auditory hallucinations in first-episode psychosis. *Hum. Brain Mapp.* 37, 1051–1065
56. Liu, Z. *et al.* (2021) Resolving heterogeneity in schizophrenia through a novel systems approach to brain structure: individualized structural covariance network analysis. *Mol. Psychiatry* 26, 7719–7731
57. Mahjoub, I. *et al.* (2018) Brain multiplexes reveal morphological connectional biomarkers fingerprinting late brain dementia states. *Sci. Rep.* 8, 4103
58. Lisowska, A. and Rekik, I. (2019) Joint pairing and structured mapping of convolutional brain morphological multiplexes for early dementia diagnosis. *Brain Connect.* 9, 22–36
59. Li, Y. *et al.* (2023) Classification of major depression disorder via using minimum spanning tree of individual high-order morphological brain network. *J. Affect. Disord.* 323, 10–20
60. Li, Y.L. *et al.* (2023) Cross-modality comparison between structural and metabolic networks in individual brain based on the Jensen-Shannon divergence method: a healthy Chinese population study. *Brain Struct. Funct.* 228, 761–773
61. Hansen, J.Y. *et al.* (2023) Integrating multimodal and multiscale connectivity blueprints of the human cerebral cortex in health and disease. *PLoS Biol.* 21, e3002314
62. Van Dijk, K.R. *et al.* (2012) The influence of head motion on intrinsic functional connectivity MRI. *NeuroImage* 59, 431–438
63. Power, J.D. *et al.* (2012) Spurious but systematic correlations in functional connectivity MRI networks arise from subject motion. *NeuroImage* 59, 2142–2154
64. Baum, G.L. *et al.* (2018) The impact of in-scanner head motion on structural connectivity derived from diffusion MRI. *NeuroImage* 173, 275–286
65. Pardoe, H.R. and Martin, S.P. (2022) In-scanner head motion and structural covariance networks. *Hum. Brain Mapp.* 43, 4335–4346
66. Hu, F. *et al.* (2023) Image harmonization: a review of statistical and deep learning methods for removing batch effects and evaluation metrics for effective harmonization. *NeuroImage* 274, 120125
67. Seiger, R. *et al.* (2018) Cortical thickness estimations of freesurfer and the CAT12 toolbox in patients with Alzheimer's disease and healthy controls. *J. Neuroimaging* 28, 515–523
68. Palumbo, L. *et al.* (2019) Evaluation of the intra- and inter-method agreement of brain MRI segmentation software packages: a comparison between SPM12 and FreeSurfer v6.0. *Phys. Med.* 64, 261–272
69. Singh, M.K. (2023) Reproducibility and reliability of computing models in segmentation and volumetric measurement of brain. *Ann. Neurosci.* 0, 097275312311599
70. Bethlehem, R.A.I. *et al.* (2022) Brain charts for the human lifespan. *Nature* 604, 525–533
71. Fenchel, D. *et al.* (2020) Development of microstructural and morphological cortical profiles in the neonatal brain. *Cereb. Cortex* 30, 5767–5779
72. Wang, Y. *et al.* (2023) Age-related differences of cortical topology across the adult lifespan: evidence from a multisite MRI study with 1427 individuals. *J. Magn. Reson. Imaging* 57, 434–443
73. Shigemoto, Y. *et al.* (2023) Age and sex-related effects on single-subject gray matter networks in healthy participants. *J. Pers. Med.* 13, 419
74. Galdi, P. *et al.* (2020) Neonatal morphometric similarity mapping for predicting brain age and characterizing neuroanatomic variation associated with preterm birth. *Neuroimage Clin.* 25, 102195
75. Shigemoto, Y. *et al.* (2021) Gray matter structural networks related to 18F-THK5351 retention in cognitively normal older adults and Alzheimer's disease patients. *Eneurologicalsci* 22, 100309
76. Tijms, B.M. *et al.* (2013) Single-subject grey matter graphs in Alzheimer's disease. *PLoS One* 8, e58921
77. Tijms, B.M. *et al.* (2018) Gray matter networks and clinical progression in subjects with predementia Alzheimer's disease. *Neurobiol. Aging* 61, 75–81
78. Vermunt, L. *et al.* (2020) Single-subject grey matter network trajectories over the disease course of autosomal dominant Alzheimer's disease. *Brain Commun.* 2, fcaa102
79. Tijms, B.M. *et al.* (2014) Single-subject gray matter graph properties and their relationship with cognitive impairment in early- and late-onset Alzheimer's disease. *Brain Connect.* 4, 337–346
80. Verfaillie, S.C. *et al.* (2018) A more randomly organized grey matter network is associated with deteriorating language and global cognition in individuals with subjective cognitive decline. *Hum. Brain Mapp.* 39, 3143–3151
81. Zhao, K. *et al.* (2022) Regional radiomics similarity networks reveal distinct subtypes and abnormality patterns in mild cognitive impairment. *Adv. Sci.* 9, 2104538
82. Xu, X. *et al.* (2021) Morphological, structural, and functional networks highlight the role of the cortical-subcortical circuit in individuals with subjective cognitive decline. *Front. Aging Neurosci.* 13, 688113
83. Xu, X. *et al.* (2022) Altered pattern analysis and identification of subjective cognitive decline based on morphological brain network. *Front. Aging Neurosci.* 14, 965923
84. Casas-Roma, J. *et al.* (2022) Applying multilayer analysis to morphological, structural, and functional brain networks to identify relevant dysfunction patterns. *Netw. Neurosci.* 6, 916–933
85. Zhao, W. *et al.* (2020) Functional, anatomical, and morphological networks highlight the role of basal ganglia-thalamus-cortex circuits in schizophrenia. *Schizophr. Bull.* 46, 422–431
86. Fleischer, V. *et al.* (2023) Prognostic value of single-subject grey matter networks in early multiple sclerosis. *Brain*, Published online August 29, 2023. https://doi.org/10.1093/brain/awad288
87. Su, S. *et al.* (2023) Evaluation of individual-based morphological brain network alterations in children with attention-deficit/hyperactivity disorder: a multi-method investigation. *Eur. Child Adolesc. Psychiatry* 32, 2281–2289
88. Peng, L. *et al.* (2022) Rich-Club organization disturbances of the individual morphological network in subjective cognitive decline. *Front. Aging Neurosci.* 14, 834145
89. Homan, P. *et al.* (2019) Structural similarity networks predict clinical outcome in early-phase psychosis. *Neuropsychopharmacology* 44, 915–922
90. Li, X. *et al.* (2019) Altered topological characteristics of morphological brain network relate to language impairment in high genetic risk subjects and schizophrenia patients. *Schizophr. Res.* 208, 338–343
91. Morgan, S.E. *et al.* (2019) Cortical patterning of abnormal morphometric similarity in psychosis is associated with brain expression of schizophrenia-related genes. *Proc. Natl. Acad. Sci. U. S. A.* 116, 9604–9609
92. Shen, D. *et al.* (2021) The deficits of individual morphological covariance network architecture in schizophrenia patients with and without violence. *Front. Psychiatry* 12, 777447
93. Zhang, W. *et al.* (2020) Brain gray matter network organization in psychotic disorders. *Neuropsychopharmacology* 45, 666–674
94. Chen, T. *et al.* (2017) Anomalous single-subject based morphological cortical networks in drug-naive, first-episode major depressive disorder. *Hum. Brain Mapp.* 38, 2482–2494
95. Gao, J. *et al.* (2023) Classification of major depressive disorder using an attention-guided unified deep convolutional neural network and individual structural covariance network. *Cereb. Cortex* 33, 2415–2425
96. Li, J. *et al.* (2021) Cortical structural differences in major depressive disorder correlate with cell type-specific transcriptional signatures. *Nat. Commun.* 12, 1647
97. Zhang, T. *et al.* (2020) Subthreshold depression may exist on a spectrum with major depressive disorder: evidence from gray matter volume and morphological brain network. *J. Affect. Disord.* 266, 243–251
98. Zhao, Y. *et al.* (2020) Aberrant gray matter networks in non-comorbid medication-naive patients with major depressive disorder and those with social anxiety disorder. *Front. Hum. Neurosci.* 14, 172
99. Qiu, X. *et al.* (2023) Aberrant single-subject morphological brain networks in first-episode, treatment-naive adolescents with major depressive disorder. *Psychoradiology* 3, kkad017

100. Wu, B. *et al.* (2023) Altered single-subject gray matter structural networks in first-episode drug-naive adolescent major depressive disorder. *Psychiatry Res.* 329, 115557
101. Corps, J. and Rekik, I. (2019) Morphological brain age prediction using multi-view brain networks derived from cortical morphology in healthy and disordered participants. *Sci. Rep.* 9, 9676
102. Gao, J. *et al.* (2021) Multisite autism spectrum disorder classification using convolutional neural network classifier and individual morphological brain networks. *Front. Neurosci.* 14, 629630
103. He, C. *et al.* (2021) Individual-based morphological brain network organization and its association with autistic symptoms in young children with autism spectrum disorder. *Hum. Brain Mapp.* 42, 3282–3294
104. Yi, T. *et al.* (2022) Individual brain morphological connectome indicator based on jensen–shannon divergence similarity estimation for autism spectrum disorder identification. *Front. Neurosci.* 16, 952067
105. Ota, M. *et al.* (2021) Structural brain network differences in bipolar disorder using with similarity-based approach. *Acta Neuropsychiatr.* 33, 121–125
106. Yang, J. *et al.* (2022) A preliminary study of the effects of mindfulness-based cognitive therapy on structural brain networks in mood-dysregulated youth with a familial risk for bipolar disorder. *Early Interv. Psychia.* 16, 1011–1019
107. Collorone, S. *et al.* (2020) Single-subject structural cortical networks in clinically isolated syndrome. *Mult. Scler. J.* 26, 1392–1401
108. Yang, Y. *et al.* (2023) Cerebellar connectome alterations and associated genetic signatures in multiple sclerosis and neuromyelitis optica spectrum disorder. *J. Transl. Med.* 21, 1–14
109. Shigemoto, Y. *et al.* (2021) Single-subject gray matter networks in temporal lobe epilepsy patients with hippocampal sclerosis. *Epilepsy Res.* 177, 106766
110. Zhang, W. *et al.* (2022) A comparison of three brain atlases for temporal lobe epilepsy prediction. *J. Med. Biol. Eng.* 42, 11–20
111. Zhang, W. *et al.* (2023) Distinguishing patients with MRI-negative temporal lobe epilepsy from normal controls based on individual morphological brain network. *Brain Topogr.* 36, 554–565
112. Chen, Y. *et al.* (2022) Altered single-subject gray matter structural networks in drug-naïve attention deficit hyperactivity disorder children. *Hum. Brain Mapp.* 43, 1256–1264
113. Chen, Y. *et al.* (2023) Altered single-subject gray matter structural networks in social anxiety disorder. *Cereb. Cortex* 33, 3311–3317
114. Zhang, X. *et al.* (2023) Disrupted brain gray matter connectome in social anxiety disorder: a novel individualized structural covariance network analysis. *Cereb. Cortex* 33, 9627–9638
115. Suo, X. *et al.* (2021) Topologically convergent and divergent morphological gray matter networks in early-stage Parkinson's disease with and without mild cognitive impairment. *Hum. Brain Mapp.* 42, 5101–5112
116. Suo, X. *et al.* (2021) Disrupted morphological grey matter networks in early-stage Parkinson's disease. *Brain Struct. Funct.* 226, 1389–1403
117. Niu, R. *et al.* (2018) Reduced local segregation of single-subject gray matter networks in adult PTSD. *Hum. Brain Mapp.* 39, 4884–4892
118. Niu, R. *et al.* (2018) Disrupted grey matter network morphology in pediatric posttraumatic stress disorder. *Neuroimage Clin.* 18, 943–951